Dynamically adjustable annular laser trapping based on axicons

Bing Shao, Sadik C. Esener, Jaclyn M. Nascimento, Elliot L. Botvinick, and Michael W. Berns

To study the chemotactic response of sperm to an egg and to characterize sperm motility, an annular laser trap based on axicons is designed, simulated with the ray-tracing tool, and implemented. The diameter of the trapping ring can be adjusted dynamically for a range of over 400 μm by simply translating one axicon along the optical axis. Trapping experiments with microspheres and dog sperm demonstrate the feasibility of the system, and the power requirement agrees with theoretical expectation. This new type of laser trapping could provide a prototype of a parallel, objective, and quantitative tool for animal fertility and biotropism study.

OCIS codes: 140.7010, 170.4520.

1. Introduction

With the deterioration of the environment and an increasing economic interest in animal husbandry, artificial insemination has become indispensable. It brings enormous economic benefit to various animal farms including fish farms, as well as helps zoological societies to save endangered species. To make artificial insemination more effective, fertility experts grade sperm according to their overall quality before freezing them for future use. Among many factors involved in the expression of sperm quality grading, initial motility score (IMS) [i.e., the product of initial motility (MOT%) and the square of speed of progression (SOP) score[1]], and hyperactivity (i.e., a distinctive motility pattern of sperm characterized by vigorous flagellar movements essential for fertilization[2]), play the two most important roles. Noninvasive and high throughput analysis of sperm motility and hyperactivity is of great significance for artificial insemination and genetic improvement programs. Conventional techniques evaluate the sperm subjectively, qualitatively on a one-by-one basis, which are labor intensive and short of a universal standard. These considerations give rise to a strong need for an automated quantitative and objective assessment tool for sperm quality. In the past decade, computer-aided sperm analysis (CASA) was developed to offer objective assessment of sperm motility for a large population. However, the thin chambers (30 μm) used in CASA impact the behavior of sperm swimming with large transverse amplitude (e.g., monkey sperm),[3] and the errors encountered by CASA when dealing with phase contrast images often misinterprets the actual sperm count in the field. Finally, while CASA can measure the motility of sperm, the force information potential useful in sperm viability assessment is lost.

Laser trapping in the near-infrared regime is a noninvasive and microfluidic-compatible biomedical tool, which has been widely applied for the physiological study of biological cells[4,5] and organelles.[6] Since the late 1980s, researchers have been using single spot laser tweezers to trap individual sperm and quantitatively evaluate the motile force generated by a sperm while it is swimming.[7,8] With the aid of laser tweezers, the relationship between sperm motility and swimming pattern was revealed,[8] and the medical aspects of sperm activity were investigated.[9,10]

Single spot laser trapping provides a quantitative analysis of individual sperm motility, nevertheless it has several drawbacks. One example is the interference from untrapped sperm. When a sperm of interest is caught by the laser tweezers, it needs to be held for a time sufficiently long for motility analysis [Figs. 1(a) and 1(b)]. However, frequently, a second sperm swims through the trapping spot, and invalidates the

B. Shao (bshao@soliton.ucsd.edu) and S. C. Esener are with the Department of Electrical and Computer Engineering, University of California, San Diego, 9500 Gilman Drive, La Jolla, California 92093-0408. J. M. Nascimento, E. L. Botvinick, and M. W. Berns are with the Department of Bioengineering, University of California, San Diego, 9500 Gilman Drive, La Jolla, California 92093-0412.

Received 16 December 2005; accepted 23 March 2006; posted 30 March 2006 (Doc. ID 66611).

0003-6935/06/256421-08$15.00/0

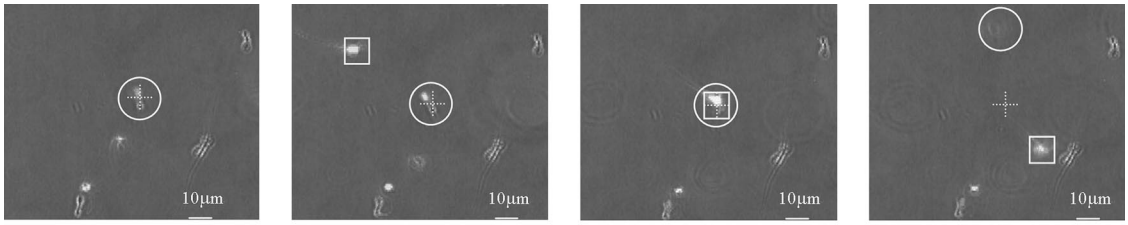

Fig. 1. Interference to single trap sperm analysis introduced by nontargeted sperm. (a) Sperm (inside the white circle) is trapped by a single spot laser trap (indicated by the white-dotted cross hair) for analysis. (b) Second sperm (inside the white square) swims toward the trapping spot. (c) Second sperm swims into the trapping spot, and interferes with the analysis of the first trapped sperm. (d) Both sperm swim out of the trap.

measurement [Figs. 1(c) and 1(d)]. Additionally, a single point laser trap still analyzes sperm one by one, which makes large-quantity evaluation time consuming and lacks the ability of *in situ* sorting based on motility and hyperactivity. Finally, single point laser trapping has difficulty in assessing the role of chemotaxis—a critical feature of sperm in response to the diffusion gradient of chemicals released by the egg and surrounding cells of the cumulus oophorus, which may help to explain infertility and provide new approaches to contraception.[11]

In this paper, a dynamically resizable annular laser trap is introduced and demonstrated, which can not only serve as a force shield to protect the analytical field from other sperm [Fig. 2(a)], but also enable multilevel parallel sorting and separation of sperm according to their motility and chemotaxis response [Figs. 2(b) and 2(c)]. The advantage of a ring trap over a single point trap or line trap lies in its ability to provide an equal-distance (from the center) condition, which is important for biological tropism study in which chemical stimuli may diffuse radially from a point source. When an attractant is fixed in the center of the ring, laser power or ring diameter can be adjusted so that only sperm swimming with sufficient energy and sensitivity to the attractant's local concentration gradient will have enough energy to pass the trap and reach the attractant. We expect that this new method of optical trapping will result in high efficiency and high throughput in a variety of biotropism (phototaxis, geotaxis, galvanotaxis, for example) studies.

There are several different ways to create an annular trap. With mechanical scanning, a ring could be generated with a fast scanning focus spot. However, this reduces the average exposure time and introduces a tangential drag force that might affect the sperm. Diffractive optics and holography generally have low-power efficiency, which is an important consideration in sperm trapping, because a single sperm trap requires 100–200 mW at the specimen plane.[12] A computer generated hologram (CGH) capable of flexibly changing the ring size and trapping depths requires a high-resolution spatial light modulator. In contrast, an axicon, also known as a conical lens or rotational symmetrical prism, has low-cost, negligible energy loss, and high flexibility. Based on these advantages, the annular laser trap was built with axicon optics.

2. Design of the Optical System

A. Annular Laser Trap

According to earlier research,[5] the deviation of the trapping spot from the optical axis is almost linearly proportional to the inclination angle θ of the input

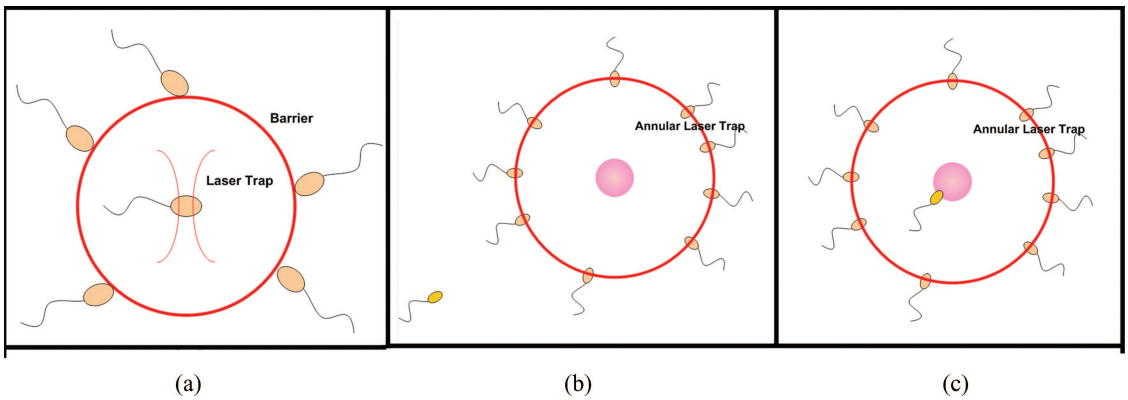

Fig. 2. (Color online) Applying a ring-shaped laser trap to facilitate sperm analysis. (a) Ring trap works as a force shield to protect sperm held by a single point laser trap from interference introduced by other untrapped sperm. (b) In sperm motility and chemotaxis research, weak sperm with low swimming power and response to central attractant are held back by the optical gradient field of the ring trap. (c) Sperm with a strong response to the central attractant develops an above-threshold swimming force to pass through the ring trap and reach the attractant in the center of the ring.

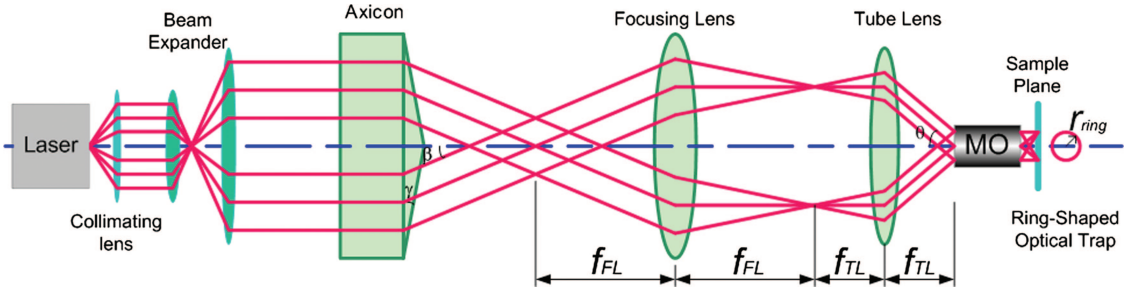

Fig. 3. (Color online) Schematic of the optics designed for annular laser trapping (not to scale); MO, microscope objective.

collimated beam. A uniform annular trap requires that incident light be composed of collimated beams from all directions (0°–360° azimuthal angle) with the same angle to the optical axis, i.e., the input light is a cone of collimated beam intersecting the back aperture of the objective. The thickness of the cone should be equal to the diameter of the back aperture so that the numerical aperture of the objective is fully utilized, and the beams are focused tightly enough to guarantee high gradient force.

The above considerations of the annular trapping system are summarized in Fig. 3 as the schematic of the annular trapping system. The laser beam is collimated, expanded by a telescope lens pair, and directed normally to the flat surface of an axicon. As a lens composed of a flat surface and a conical surface, an axicon bends normal-incident light toward its tip without affecting its degree of collimation. The beam emerging from the conical surface of the axicon is bent toward the optical axis at an angle $\beta = \arcsin(n \sin\gamma) - \gamma$, where γ is the base angle of the axicon and n is the refractive index of the lens material. A focusing lens converts the cone of collimated beams into a ring, which is then imaged in the specimen plane via the tube lens–objective combination.

Since the focusing lens and the tube lens work together as a telescope, the inclination angle of the light beams incident on the objective is $\theta = \beta f_{FL}/f_{TL}$, where f_{FL} and f_{TL} are the focal lengths of the focusing lens and the tube lens, respectively. Accordingly, the radius of the ring trap can be calculated as

$$r_{ring} = \delta = f_{EFL}\tan(\theta) = f_{EFL}\tan\left(\frac{f_{FL}}{f_{TL}}\beta\right) = f_{EFL}\tan\left\{\frac{f_{FL}}{f_{TL}}[\arcsin(n\sin\gamma) - \gamma]\right\}, \quad (1)$$

where f_{EFL} is the effective focal length of the microscope objective.

To obtain high-power throughput for the 1070 nm trapping wavelength, the laser beam is directed to the objective through the epifluoresence port of an inverted microscope (Axiovert 200M, Zeiss, Germany) with the arc lamp tube system removed. In this way, a 1064 nm antireflection- (AR) coated plano–convex singlet lens (f_{TL} = 400 mm, KPX208AR.18, Newport, Irvine, California) is used instead of the microscope-embedded tube lens that is AR-coated for visible light. A 1 in. (2.54 cm) BK7 (n = 1.506) axicon lens with broadband AR coating and base angle γ = 10° (Del Mar Photonics, San Diego, California) is chosen so that together with the focusing lens (f_{FL} = 100 mm, KPX187AR.18), the tube lens and the microscope objective (EC Plan-Neofluar, DIC, 40× NA = 1.3, oil immersion, Zeiss, Germany), a ring trap with a diameter of hundreds of micrometers could be formed.

Ray-tracing simulations (ZEMAX, Bellevue, Washington) with a plane-wave input show a sharp and uniform ring focus on the specimen plane [in Figs. 4(b)–4(d)]. Although some rays fail to focus due to the off-axis aberration coma, both the spot diagram [Fig. 4(b)] and the cross section [Fig. 4(c)] show that they only occupy a negligible percentage of the light. The Huygens point-spread function (PSF) cross section in the transverse plane in Fig. 4(d) shows two intensity peaks with a high gradient, indicating a strong gradient force on the specimen plane. The radius of the ring obtained from the spot diagram simulation [Fig. 4(b)] is about 210 μm, which agrees well with the calculation.

B. Diameter-Adjustable Annular Laser Trap

The faster a sperm swims, the higher the laser power is needed for trapping. With the total input power fixed, diameter changes of the annular trap lead to a variation of trapping powers per spot. As a result, sperm with different motility will escape the trap at different times. Thus multilevel sorting is allowed. Additionally, since the size of sperm may vary between species, resizability of the system makes it possible to study different species without redesigning the optics. Finally, a resizable ring can be used to study the diffusion length of an attractant.

The size of the ring focus is determined by the apex angle of the input light cone (θ in Figs. 3 and 5). To change this angle dynamically without changing the thickness of the cone that corresponds to the filling degree of the objective back aperture, two more axicons are added (Axi2 and Axi3 in Fig. 5). The ability of an axicon to bend incoming light without changing its collimation degree makes it the right choice. When a normal telescope lens pair is used, however, the changing of θ is accompanied by a change of the beam size, which will

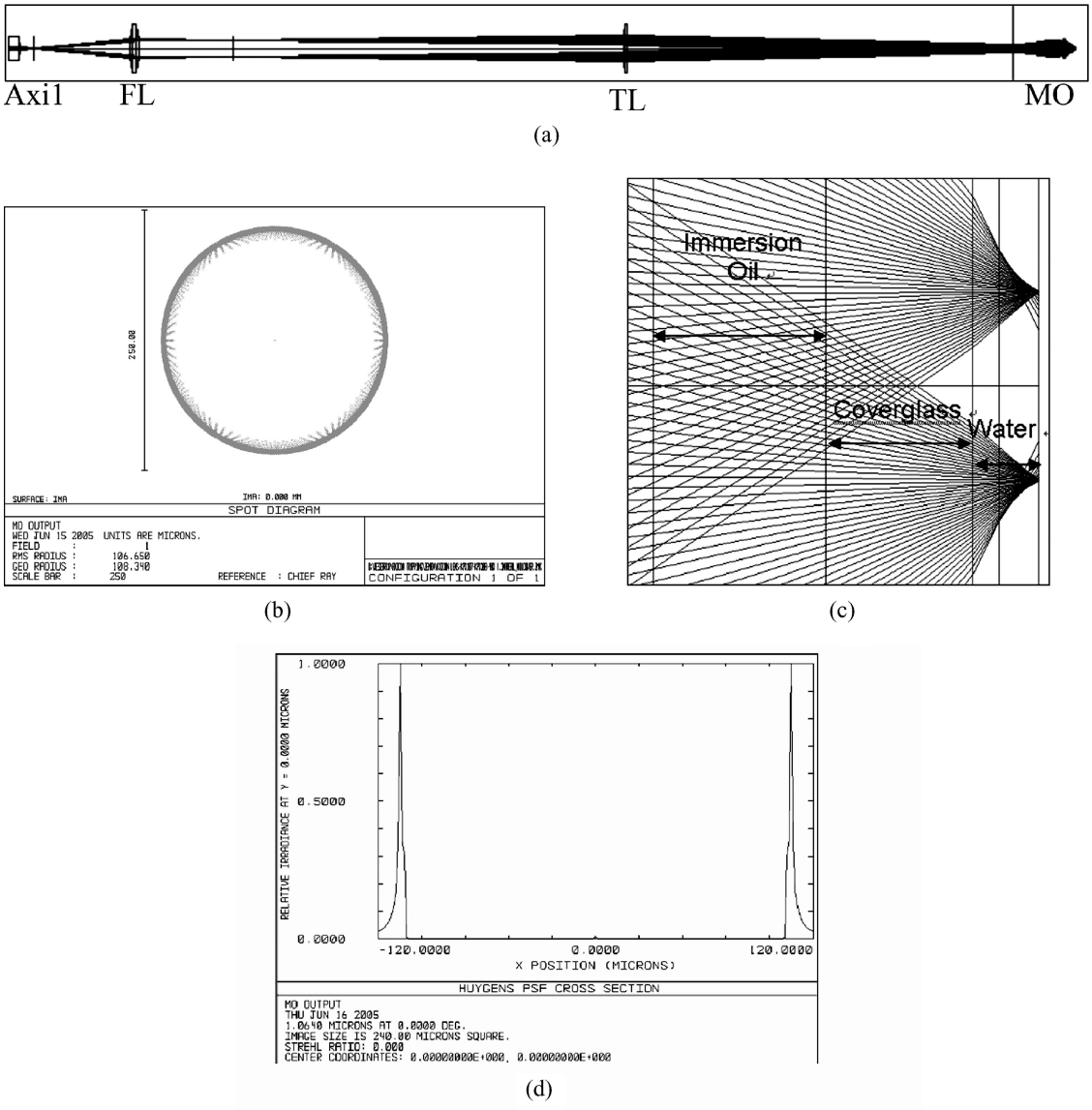

Fig. 4. ZEMAX simulations of an axicon-based ring-trap system. (a) System layout. (b) Spot diagram at the specimen plane shows the size and quality of the ring focus. (c) Closeup of the system layout near the specimen plane gives a cross-sectional view of the ring focus formation; only a negligible amount of rays failed to focus due to coma. (d) Huygens PSF cross section shows a strong gradient of light intensity on the specimen plane. Axi1, axicon 1; FL, focusing lens; TL, tube lens; MO, microscope objective.

result in an overfilling or underfilling of the objective back aperture. ZEMAX simulations with a 40× NA of 1.30 oil immersion objective, $f_{FL} = 100$ mm, $f_{TL} = 400$ mm show that, with all other elements fixed, axial translating Axi2 for 80 mm corresponds to a ring diameter change from 84 μm [Fig. 5(a)] to 486 μm [Fig. 5(b)].

3. Experimental Result

A. Experimental Setup

The experimental setup is shown in Fig. 6. The light beam from a fiber laser with 1070 nm wavelength (PYL-20M, IPG Photonics, Oxford, Massachusetts) is collimated and expanded via a telescope lens pair. Upon the axicon, the input beam is divided with respect to the optical axis and bent toward it at an angle of $\beta = 5.16°$. The back focal plane of the axicon conjugates with the back aperture of the microscope objective. At the same time, the back focal plane of the focusing lens conjugates with the specimen plane.

B. Experiments with Microspheres

Experiments with 15 μm diameter polystyrene microspheres (2015A, Duke Scientific, Palo Alto, California) were carried out to demonstrate the feasibility of an annular trap. A microsphere-water suspension is put into a plastic dish with a 0.017 mm thick glass coverslip as the bottom (P35G-1.5-14-C, MatTek, Ashland, Massachusetts). Under a postobjective power of 80 mW, a full ring of microspheres is created along the fine annular focus (Fig. 7). The diameter of the ring is

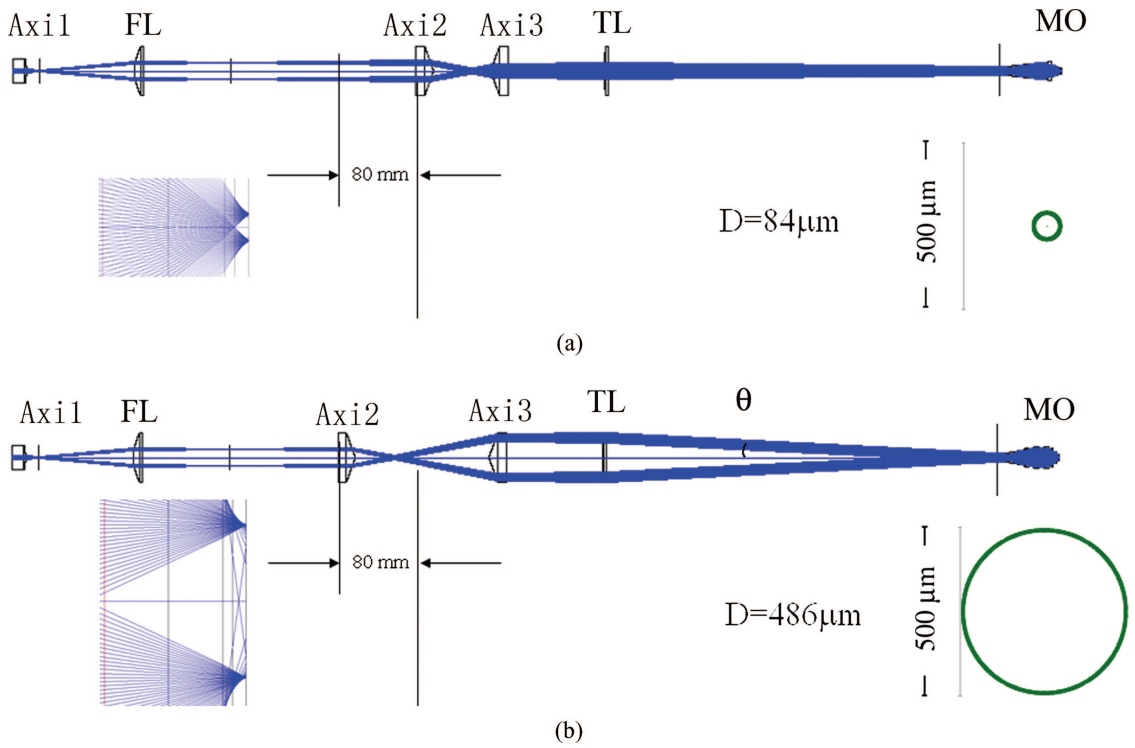

Fig. 5. (Color online) ZEMAX simulations of an adjustable annular laser trap with a 40× NA of 1.30 oil immersion objective. (a) Layout, focus closeup, and sample plane spot diagram for minimal ring size, (b) layout, focus closeup, and sample plane spot diagram for maximal ring size. Axi1, axicon 1; Axi2, axicon 2; Axi3, axicon 3.

about 210 μm, which agrees well with the calculation and simulation results. Under the assumption of uniform power distribution along the ring, the average trapping power per microsphere was estimated to be 2.4 mW. The bright pattern in the center is due to the scattering and internal reflection of the microscope optics at the glass–water interface as well as stray light. In Figs. 7(a) and 7(b), the leftward stage translation collects additional microspheres (initially on the right side of the ring) into the annular focus, forcing subsequent redistribution of the squeezed microspheres along the ring (as shown with the black arrows). This observation indicates a strong optical gradient in the radius direction and no confinement effect circumferentially.

The size adjustability of the annular trap is demonstrated with microspheres. Figure 8 shows the experimental results corresponding to two typical positions of Axi2. When the axial spacing between Axi2, and Axi3 is 89 mm, the annular focus obtained at the specimen plane has a diameter of 240 μm [Fig. 8(a)], whereas for axial spacing 63 mm, the diameter of the ring is reduced to 135 μm [Fig. 8(b)]. Both experimental results agree very well with the ZEMAX simulation [Figs. 8(c) and 8(d)].

C. Experiment with Dog Sperm

Dog sperm [provided by the Conservation and Research for Endangered Species (CRES), Zoological Society of San Diego, California] are stored in liquid N_2

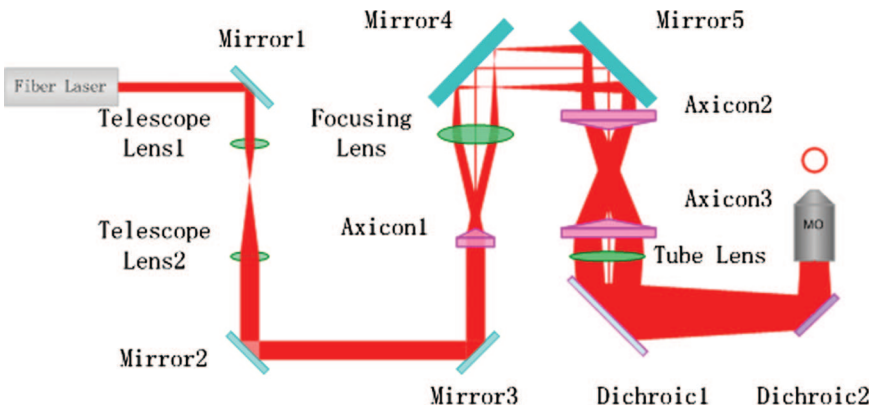

Fig. 6. (Color online) Experimental setup of the dynamically adjustable annular laser trap.

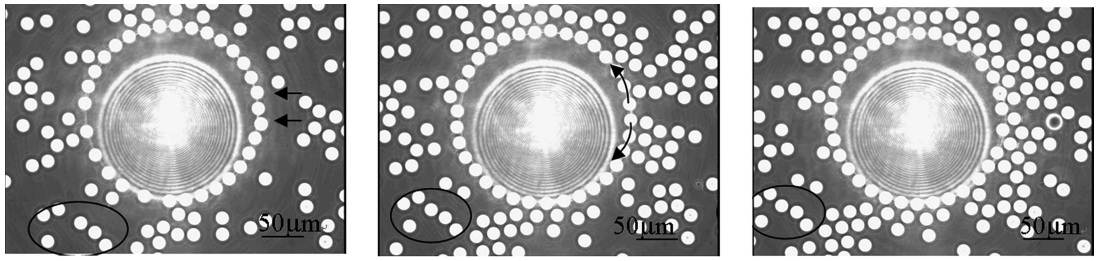

(a) (b) (c)

Fig. 7. Video frames taken from an experiment of annular laser trapping of 15 μm polystyrene spheres in water with a 40× NA of 1.30 oil immersion objective. (a) With the stage at the original position, a ring of microspheres was formed along the annular focus of the laser beam. (b) Frame taken after translating the stage to the left with a speed of 1 μm/s for 10 s. (c) Frame taken after a subsequent leftward translation of the stage with a speed of 2 μm/s for 10 s. The six beads in the white ellipse were used as a reference.

(77 K) until needed for experimentation.[13,14] After thawed in a prewarmed water bath (37 °C) for approximately 30 to 60 s, sperm are transferred to an Eppendorf tube and centrifuged at 2000 rpm for 10 min. Excess waste is removed, and the sperm pellet is resuspended in 1 mL of prewarmed Biggers–Whitten–Whittingham (BWW) and bovine serum albumin (BSA) media (1 mg of BSA per 1 mL of BWW, osmolality of 270–300 mmol/kg water, pH of 7.2–7.4).[15] Final dilutions are created from this stock solution (desired final concentration of 106,000 sperm per milliliter of BWW).

Figure 9 shows the preliminary result of an experiment with a 110 μm diameter ring on dog sperm. Under the power of approximately 70 mW/sperm, nonmotile sperm and red blood cells are stably trapped along the ring [Figs. 9(a)–9(d)], slow sperm get drawn to the ring and scattered, whereas fast ones and those not in the trapping plane are barely affected. This is consistent with the fact that approximately 70–100 mW is needed to trap a slow sperm.[12] Although system optimization is necessary to get better trapping stability in the axial direction, and higher power is needed to affect fast sperm, these

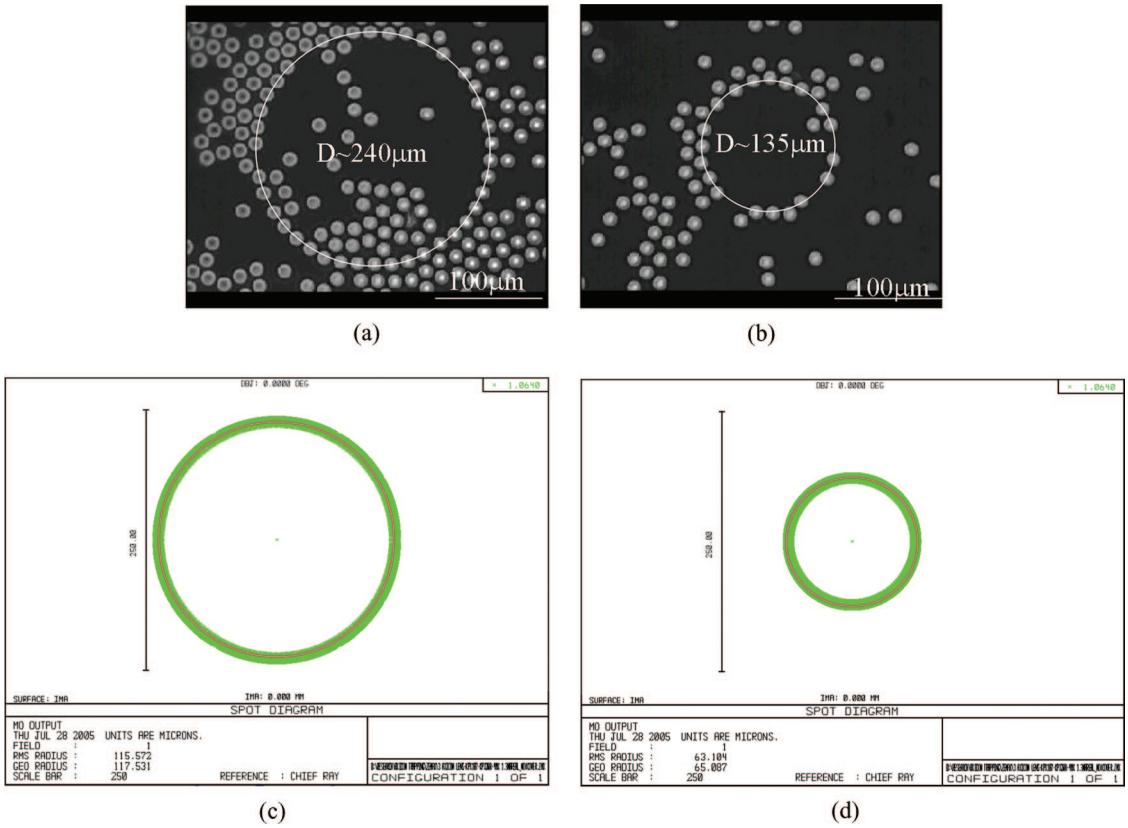

(a) (b) (c) (d)

Fig. 8. (Color online) Annular trapping of 15 μm microspheres for two typical axial positions of Axi2, experiments and simulations. (a) Video frame taken from the experiment when the distance between Axi2 and Axi3 is $d = 89$ mm; (b) video frame taken from experiment when the distance between Axi2 and Axi3 is $d = 63$ mm; (c) ZEMAX-simulated spot diagram at a specimen plane for $d = 89$ mm; and (d) ZEMAX-simulated spot diagram at a specimen plane for $d = 63$ mm.

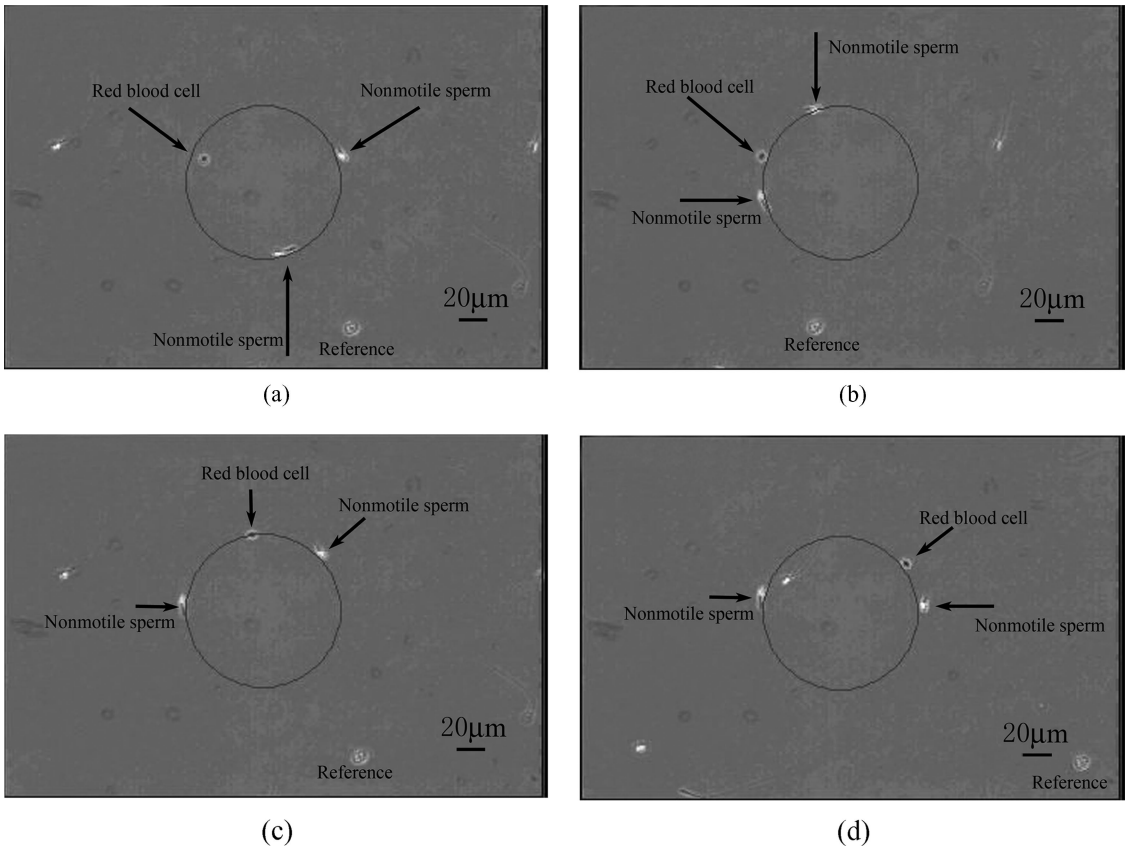

Fig. 9. Video frames from an experiment with dog sperm. (a) Frame #340; (b) Frame #360, stage is moved leftward with respect to Frame #340; (c) Frame #380, stage is moved rightward with respect to Frame #360; (d) Frame #400, stage is moved further right.

results give an idea of the parallelism a ring trap can provide to sperm analysis, and the varied response to the ring from sperm with different motilities.

4. Conclusion

A dynamically adjustable annular laser trap was designed and built using axicons. By simply translating one of the axicons along the axis, the diameter of the ring can be changed for a range of over 400 μm. Simulation shows a sharp and uniform annular focus on the specimen plane, whose diameter agrees well with both the theoretical calculation and the experimental measurement, and the high-intensity gradient which indicates a strong trapping force. Experiments with microspheres demonstrate the feasibility of the ring trap. Preliminary experiments on actively swimming dog sperm show the parallelism provided by the ring trap in cell analysis and different responses to the ring from sperm with different motility. Further optimization of the system is necessary to ensure a strong enough gradient force in three dimensions for slowing down or trapping fast swimming sperm. This could be achieved by using a top-hat beam profile and replacing the current glass-bottom dish with a thin chamber (thickness <200 μm), because the thicker the chamber the more convection flow is introduced, which would add perturbation to the laser trap, especially in the axial direction.

We believe the system provides a prototype of an objective, parallel, and quantitative analytical tool for studies on biotropism and cell dynamics (including animal fertility).

The authors thank Scripps Institute of Oceanography for financial support, Barbara Durrant of the Zoological Society of San Diego, and the Beckman Center for Conservation and Research for Endangered Species for the dog sperm.

References

1. B. Durrant, D. Amodeo, A. Anderson, and M. A. Olson, "Effect of extraction methods on cryopreservation of canine epididymal sperm," in *Society for the Study of Reproduction 33rd Annual Meeting, 15–18 July 2000,* (Madison, Wisc., 2000), BAR-4-5-3.
2. H. Schmidt and G. Kamp, "Induced hyperactivity in boar spermatozoa and its evaluation by computer-assisted sperm analysis," Reproduction **128,** 171–179 (2004).
3. J. Baumber and S. A. Meyers, "Hyperactivated motility in rhesus macaque (*Macaca mulatta*) spermatozoa," J. Androl. **27,** 459–468 (2006).
4. M. Ozkan, M. M. Wang, C. Ozkan, R. A. Flynn, and S. Esener, "Optical manipulation of objects and biological cells in microfluidic devices," Biomed. Microdevices **5,** 47–54 (2003).
5. B. Shao, S. Zlatanovic, and S. C. Esener, "Microscope-integrated micromanipulation based on multiple VCSEL traps," in *Optical Trapping and Optical Manipulation,* K. Dholakia and G. C. Spalding, eds., Proc. SPIE **5514,** 62–72 (2004).

6. M. W. Berns, "Laser scissors and tweezers," Sci. Am. (Int. Ed.) **278,** 52–57 (1998).
7. Y. Tadir, W. H. Wright, O. Vafa, T. Ord, R. H. Asch, and M. W. Berns, "Micromanipulation of sperm by laser generated optical trap," Fertil. Steril. **52,** 870–873 (1989).
8. Y. Tadir, W. H. Wright, O. Vafa, T. Ord, R. H. Asch, and M. W. Berns, "Force generated by human sperm correlated to velocity and determined using a laser generated optical trap," Fertil. Steril. **53,** 944–947 (1990).
9. P. Patrizio, Y. Liu, G. J. Sonek, M. W. Berns, and Y. Tadir, "Effect of pentoxifylline on the intrinsic swimming forces of human sperm assessed by optical tweezers," J. Androl. **21,** 753–756 (2000).
10. Z. N. Dantas, E. Araujo, Jr., Y. Tadir, M. W. Berns, M. J. Schell, and S. C. Stone, "Effect of freezing on the relative escape force of sperm as measured by a laser optical trap," Fertil. Steril. **63,** 185–188 (1995).
11. M. Eisenbach and I. Tur-Kaspa, "Do human eggs attract spermatozoa?" BioEssays **21,** 203–210 (1999).
12. J. M. Vinson, E. L. Botvinick, B. Durrant, and M. W. Berns, "Correlation of sperms' swimming force to their swimming speed assessed by optical tweezers," in *Optical Trapping and Optical Micromanipulation II,* K. Dholakia and G. C. Spalding, eds., Proc. SPIE **5930,** 593026 (2005).
13. S. A. Harper, B. S. Durrant, K. D. Russ, and D. Bolamba, "Cryopreservation of domestic dog epididymal sperm: a model for the preservation of genetic diversity," J. Androl. **19,** (Suppl.), 50 (1998).
14. B. S. Durrant, S. A. Harper, D. Amodeo, and A. Anderson, "Effects of freeze rate on cryosurvival of domestic dog epididymal sperm," J. Androl. **21** (Suppl.), 59 (2000).
15. J. D. Biggers, W. K. Whitten, and D. G. Whittingham, "The culture of mouse embryos in vitro," in *Methods in Mammalian Embryology*, J. C. Daniels, ed. (Freeman, 1971), pp. 86–116.